Eikonal Solver In The Celerity Domain

Linbin Zhang*

Earth Sciences Division, Lawrence Berkeley National Laboratory, Berkeley, CA94720, USA

James W. Rector III

Department of Civil and Environmental Engineering, University of California, Berkeley, CA 94720-1710, USA

G. Michael Hoversten

Earth Sciences Division, Lawrence Berkeley National Laboratory, Berkeley, CA94720, USA

* Formerly at Department of Material Science and Engineering, University of California, Berkeley, CA 94720-1760, USA

SUMMARY

A finite-difference method for computing the first arrival traveltimes by solving the Eikonal equation in the celerity domain has been developed. This algorithm incorporates the head and diffraction wave. We also adapt a fast sweeping method, which is extremely simple to implement in any number of dimensions, to obtain accurate first arrival times in complex velocity models. The method, which is stable and computationally efficient, can handle instabilities due to caustics and provide head waves traveltimes. Numerical examples demonstrate that the celerity-domain Eikonal solver provides accurate first arrival traveltimes. This new method is three times accurate more than the 2^{nd}-order fast marching method in a linear velocity model with the same spacing.

Key words: finite-difference methods, traveltime, fast sweeping method.

1 INTRODUCTION

The finite difference (FD) approximation to the Eikonal equation was introduced by Reshef and Kosloff (1986) and Vidale (1988,1990) for calculating traveltimes through a 2D or 3D velocity model. This method is much faster than tracing rays from a large number of sources to a large number of receivers because the traveltimes for all grid points within a model are computed at the same time. It may be used for 2D or 3D depth migration, tomography or velocity analysis.

When compared with analytic solutions, eikonal solvers exhibit some degree of traveltime error, which may lead to poor image focusing in migration or inaccurate velocities estimated via tomographic inversion. For examples, Vidale's second-order FD scheme, first-order FD (Podvin and Lecomte, 1991) or Kim and Cook's (1999) second-order FD are not exact solution even for a constant velocity model. More accurate FD methods such as non-Cartesian (Alkhalifah and Fomel, 1997; Sun and Fomel, 1998 a, b), spherical grids (Fowler, 1994), triangulated grids (Kimmel and Sethian, 1998; Sethian and Vladimirsky, 2000), unstructured grids (Fomel,1997), adaptive rectangular grid (Qian and Symes,2002) and non-linear interpolation schemes (Schneider et al., 1992 and Zhao,1996) reduce inaccuracies. However the cost is more algorithmic complexity.

Pica (1997) proposed a FD method that solves the Eikonal equation in the celerity domain. He defined a variable called celerity, which is the distance from the source divided by the traveltime from the source. The celerity is an average velocity, weighted by the straight-line distance from the source, irrespective of the true ray path. The celerity transform takes into account the curvature of the isochrones approximately. Consequently, accurate traveltimes can be obtained on a coarse grid without distorting the wave-front curvature. The coarse grid enables efficient travel-time computation.

The celerity method proposed by Pica (1997) works as follows:

1) the celerity is computed analytically;

2) the spatial derivatives of the celerity are computed by FD;

3) the celerity is extrapolated downward;

4) the celerity back to the traveltimes.

The downward extrapolation used in Pica's approach cannot compute upgoing arrivals such as may be observed in complex velocity models.

In this paper, we modify Pica's method. We combine a local traveltime computation scheme in the celerity domain with a global fast sweeping method in the time domain. In the local traveltime computation scheme, we consider not only the transmitted waves, which can be calculated by FD in celerity domain, but also diffracted and head waves (Podvin and Lecomte, 1991; Afnimar and Koketsu, 2000). To take all possible wave propagations from different directions into account, a fast sweeping method (Zhao, 2003 and Tsai, et al, 2003) is used to select the 'correct' traveltime for each grid point.

Our paper is organized as follows. We first derive the eikonal equation in the celerity domain. Then local schemes are given in which FD is used to solve the new Eikonal equation and a global sweeping scheme is used to update the traveltimes. Numerical examples demonstrate the accuracy and efficiency of the method.

2 THEORY

Under a high frequency approximation, propagating wavefronts may be described by the Eikonal equation,

$$\left(\frac{\partial t}{\partial x}\right)^2 + \left(\frac{\partial t}{\partial y}\right)^2 + \left(\frac{\partial t}{\partial z}\right)^2 = S^2(x,z) \tag{1}$$

where t is the traveltime, S is the slowness, and x ,y and z represent the spatial Cartesian coordinates.

Celerity is defined as (Pica, 1997):

$$C = \frac{d}{t} = \frac{\sqrt{(x-x_s)^2 + (y-y_s)^2 + (z-z_s)^2}}{t(x,y,z)} \tag{2}$$

where (x_s, y_s, z_s) are the coordinates and t is the traveltime from the source. By change of variables, equation (1) can be written in the form:

$$\frac{d^2}{C^2}(C_x^2 + C_y^2 + C_z^2) - \frac{2}{C}((x-x_s)C_x + (y-y_s)C_y + (z-z_s)C_z) + 1 - C^2S^2 = 0 \tag{3}$$

where the subscripts attached to celerity C, the new unknown, denotes the partial derivative with respect to the spatial Cartesian variables, for instance, $C_x = \frac{\partial C}{\partial x}$.

2.1 2-D calculation

2.1.1 Local traveltime computation

From equation (3), we can compute the travel time at any grid point in a 2-D model if we know travel times at two adjacent grid points. As shown in Figure 1, the travel times at A and B are known and C is unknown. The computation scheme must be able to compute the minimum traveltime for any possible emanation position between A and B including the endpoints. We use the first order FD to approximate the first derivative. Between A and B the traveltime at C, t_c can be obtained as follows:

1) compute C_z by FD :

$$C_z = \frac{C_A - C_B}{z_A - z_B} \tag{4}$$

where $C_A = \frac{d_A}{t_A}$ and $C_B = \frac{d_B}{t_B}$.

2) compute C_x by analytically solving equation (3):

3) compute celerity C_C at C, by FD:

$$C_c = C_A + C_x(x_C - x_A) \tag{5}$$

4) inverse transform from celerity to time:

$$t_C = \frac{d_C}{C_C} \qquad (6)$$

where

$$d_C = \sqrt{(x - x_s)^2 + (z - z_s)^2}$$

To investigate the stability of this algorithm, suppose a transmitted wave passes AB to C. From Figure 1, we know that the angle, θ, between the transmitted wave and the vertical direction is:

$$\cos^{-1} \frac{dz}{\sqrt{dz^2 + dx^2}} \le \theta \le \frac{\pi}{2} \qquad (7)$$

rewriting:

$$0 \le \cos\theta \le \frac{dz}{\sqrt{dz^2 + dx^2}} \qquad (8)$$

Note that

$$\cos\theta = \frac{\frac{\partial t}{\partial z}}{S} \qquad (9)$$

Using equations (8) and (9), one can obtain:

$$0 \le t_A - t_B \le \frac{dz^2}{\sqrt{dz^2 + dx^2}} S \qquad (10)$$

As long as equation (10) is satisfied, we can use equations (4)-(6) to calculate transmission traveltimes.

If the slowness contrast across the interface, AC, is large, there may be a head wave arrival. In order to compute head wave traveltimes, we use Podvin & Lecomte's operators (Podvin & Lecomte, 1991). For a head wave,

$$t_C = t_A + \min(S, S')dx \tag{11}$$

where S and S' are the slowness in ABCD and ACGF, respectively.

For a diffraction from B to C,

$$t_C = t_B + S\sqrt{dx^2 + dz^2} \tag{12}$$

The smallest traveltime for each of these three possible emanation positions is retained for future calculations by the fast sweeping method.

2.1.2 Global computation scheme: the fast sweeping method

In the local scheme, we only consider the wave propagation from AB to C. However in complex velocity models, waves can propagate from any direction to C. As we can see in Fig.2 there are 16 possible wave propagations from A1-8 to the middle point of interest: 8 transmitted waves, 4 diffraction and 4 head waves. To simulate these possible waves, we adapt a fast sweeping method proposed by Zhao (2003) and Tsai et al (2003). Let us denote traveltime at the grid (i, j) as $t(i, j) = t(x, z) = t(i\Delta x, j\Delta z)$, $i = 1,2..., Nx$, $j = 1,2,..., Nz$, where Δx and Δz are the spacing in x and z direction, respectively. We initially assign the traveltime $t(is, js) = 0$ at source location (is, js) and very big values at other grid points $t(i, j) = \infty$ or large values. The fast sweeping method then proceeds by updating the values $t(i, j)$ in a certain order: sweeps in positive and negative X, and positive and negative Z directions.

Let $t^{current}(i, j), i = 1,2,..Nx, j = 1,2,...Nz$ denote the current traveltime at the grid (i, j). At each grid (i, j) we compute the minimum traveltime, denoted by $t^{temp}(i, j)$, by Eq. (11), (12) and the finite difference scheme from the current value of its neighbors $t^{current}(i \pm 1, j)$ and $t^{current}(i, j \pm 1)$ and then update $t(i, j)$ to be the smaller one of $t^{temp}(i, j)$ and its current value, i.e. $t(i, j) = \min(t^{current}(i, j), t^{temp}(i, j))$. We sweep the whole domain with alternating orderings repeatedly. The pseudo-code of the fast sweeping method in 2D is:

1) for $j = 1$ to Nz; for $i = 1$ to Nx; calculate $t^{temp}(i, j)$, $t(i, j) = \min(t^{current}(i, j), t^{temp}(i, j))$;
2) for $j = 1$ to Nz; for $i = Nx$ to 1; calculate $t^{temp}(i, j)$, $t(i, j) = \min(t^{current}(i, j), t^{temp}(i, j))$;
3) for $i = 1$ to Nx; for $j = 1$ to Nz; calculate $t^{temp}(i, j)$, $t(i, j) = \min(t^{current}(i, j), t^{temp}(i, j))$;
4) for $i = 1$ to Nx; for $j = Nz$ to 1; calculate $t^{temp}(i, j)$, $t(i, j) = \min(t^{current}(i, j), t^{temp}(i, j))$;
5) Go to 1) until $\max | t(i, j) - t^{temp}(i, j) | < \varepsilon$, where ε is a small number.

Using this approach, traveltimes for each point in the grid is calculated several times using the previously calculated traveltimes at surrounding grid points until the minimum time is found. Different ranges of propagation angles are covered as shown in Figure 2. This guarantees that the first-arrival traveltime for a specific grid point is correctly calculated. This fast sweeping method has an optimal complexity of O(N) for $\mathrm{N} = Nx \times Nz$ grid points while the complexity of the fast marching is of order O(NlogN) (Zhao, 2003) and is extremely simple to implement in any dimension.

2.2 3-D calculation

2.2.1 Local traveltime computation

In the 3D case, the local traveltime computation method is shown in Fig. 3. In Fig.3 (a), the travetime at point E is computed from A, B and D, in which C_x is calculated from A and D and C_y from A and B. In Fig.3 (b), the travetime at point E is computed from A, B and C, in which C_x is calculated from B and C and C_y from A and B. In Fig.3(c), the travetime at point E is computed from A, D and C, in which C_x is calculated from C and D and C_y from A and D. The celerity at point E can be computed by equation (3).

To consider head and diffraction waves, we compute the traveltime at point E by using the 2D and 1D local traveltime computation algorithm described above. In the 2D local traveltime computation algorithm, the travetime at point E is computed from A and B, from A and D, from C and D, and from B and C, respectively. In the 1D traveltime computation algorithm, we use equations (11) to compute the potential arrival traveltime at point E from A, D and B. The diffraction traveltime from point C to E can be computed by:

$$t_E = t_C + S\sqrt{dx^2 + dy^2 + dz^2} \tag{13}$$

We pick the minimum value of all potential arrivals as the first travetime at point E.

2.2.2 Global computation scheme: the fast sweeping method

The fast sweeping method can be extended to 3D space rather easily. We should sweep in positive/negative X, positive/negative Y, positive/negative Z, six directions. At each gird, we keep the minimum traveltime as first arrival time. If solution has changed little since last iteration, stop computing; else go back to sweep.

3 EXAMPLES

All examples shown below are done on a laptop with a single processor 1.2 GHz Pentium III. First, to examine the accuracy of the new algorithm, we calculated the travel times in a 3D homogenous velocity model (2500 m/s) and compare these with analytic traveltimes. For a 100m grid spacing and a 1,000,000 m^3 model, the maximum relative error is less than 0.0001. The computation time was 12s.

We also compared the method with the 2^{nd}-order fast marching method (FMM) and Vidale's algorithm using two 2D velocity models: one homogenous model with a constant velocity $V = 6\,000$ m/s and the other is a velocity model with a linear vertical gradient (Rawlinson and Sambridge, 2004). In the first model, the source is located at depth 40,000 m. There are 21 receivers on the surface with intervals 5000 m. Figure 4 shows wave fronts while Figure 5 shows the errors between the numerical and analytically computed traveltimes with spacing 1000m both in x and z directions. We found that the maximum travel time difference between the 2D FD and exact solution is 0.01 ms and the maximum relative error between the 2D FD and exact solution is 9.95×10^{-5} %. While the maximum traveltime difference between the 2nd order fast marching method (FMM) and the analytic solutions is approximately 36 ms for the same model with the same spacing 1000 m (Rawlinson and Sambridge, 2004). Vidale's algorithm with the same grid spacing has a maximum relative error between the numerical and exact solution 0.18%. Figure 6 shows the traveltime differences between the numerical and exact solution at the 21 receivers. We can see that the maximum error is –0.002 ms. The maximum traveltime difference between the 2nd order fast marching method (FMM) with the spacing 125 m for the same model and the analytic solutions at these receivers is as large as 5 ms. Therefore the accuracy of our method for homogenous models is much higher than that of the FMM and Vidale's methods. The error of our method in this constant velocity model is mainly due to round-off error.

The second example is a linear increase in velocity with depth (Rawlinson and Sambridge, 2004):

$$V(x,z) = 4000 + 0.1z \ \text{(m/s)}$$

The model is 100 km × 40 km. The source is located at (0,0). There are 21 receivers along surface with intervals 5 km. Figure 7 a) shows the wavefronts obtained by the Eikonal solver with the spacing $\Delta x = \Delta z = 125m$. The relative error between the Eikonal and the theoretical solution are shown in Figure 7 b) and the maximum relative error is 0.479%. To compare the new method with the fast marching method (Rawlinson and Sambridge, 2004) we plot the difference between numerical and analytic solutions at the 21 receivers on the surface using our FD Eikonal solver with four different grid spacings: 1000, 500, 250 and 125 m in Figure 8. For the 1000 m spacing the maximum error is 16 ms with our algorithm while that in Rawlinson and Sambridge's (2004) algorithm is as large as 60 ms. The error of our algorithm is reduced to 1.5 ms for a spacing 125 m but the error of the 2^{nd}-order FMM is still larger than 6 ms.

Figure 9 shows the rms error between numerical and analytic solutions as a function of grid spacing and a plot of CPU time against total grid points N for the linear velocity model. The time shown is elapsed (wall clock) time on a 1.2 GHz Pentium III. It can be seen from Figure 9 that the accuracy of the new method increases linearly as grid spacing decreases and the CPU time increases linearly as total grid points increases.

Figure 10 is a salt dome model. This model has been widely used to test migration algorithm such as Kirchoff and wave equation migration methods. The model is 13.5 km $\times$3.68 km. The grid spacing we used for the Eikonal solver was 20 m in X and Y. The results are shown in Figure 8. For this 605 $\times$184 cells model, calculation took 0.4 s with 4 sweeps.

4 CONCLUSIONS

We have developed a FD Eikonal equation with a fast sweeping method in the celerity domain to compute the first arrival time in arbitrarily complex media. We have shown that the new Eikonal solver in the celerity domain produces traveltimes with high accuracy. This Eikonal solver produces almost exact results in homogenous models. Our method accounts for transmission, diffraction and head waves and their propagation direction. It can overcome numerical instability of some FD methods in complex velocity models. Numerical results show that the new method is more accurate than the 2nd order fast marching method. It is shown that 4 iterations are adequate for the 2D case. This algorithm has applications in migration and seismic tomographic imaging. Numerical examples also show that the accuracy of this method increases linearly with decreasing grid spacing, make selection of a desired accuracy level predictable.

ACKNOWLEDGMENTS

We are grateful to Dr. Sergey Fomel of the Bureau of Economic Geology for reviews the manuscript and offering valuable suggestions. We also appreciate the anonymous reviews for their helpful comments. Support for this work was provided by the Assistant Secretary for Fossil Energy, through the National Energy Technology Laboratory under U.S. Department of Energy under Contract No. DE-AC03-76SF00098.

REFERENCE

Afnimar and Koketsu, K., 2000, Finite difference traveltime calculation for head waves traveling along an irregular interface, Geophys. J. Int., **143**,729-734.

Alkhalifah, T. and Fomel, S., 1997, Implementing the fast marching Eikonal solver: Spherical versus Cartesian coordinates, SEP-**95**, 149-171.

Alkhalifah, T. and Fomel, S., 2001, Implementing the fast marching Eikonal solver: Spherical versus Cartesian coordinates: Geophysical Prospecting, **49**, 165-178.

Fomel, S., 1997, A variation formulation of the fast marching Eikonal solver: SEP-**95**, 127-147.

Fowler, P.J., 1994, Finite-difference solution of the 3-D Eikonal equation in the spherical coordinates: 64th Ann. Internat. Mtg. Soc. Expl. Geophys., Expanded Abstracts, 1394-1397.

Kim, S. and Cook, R., 1999, 3-D traveltime computation using second-order ENO scheme, Geophysics, **64**, 1867-1876.

Kimmel, R., and Sethian, J.A., 1998, Fast marching methods on triangulated domains: Proc. Nat. Acad. Sci., **95**, 8341-8445.

Lecomte,I., 1993, Finite difference calculation of first traveltimes in anisotropic media: Geophys. J. Int., **113**, 318-342.

Mendes, M., Morgado, L., Buxo, A., 1997, Interpolation sensitivity of the 3D ASI: Final Report EEC Joule contract JOU2-CT93-0321, 3D Asymptotic Seismic Imaging, 251- 263.

Pica, A., 1997, Fast and accurate finite-difference solutions of the 3D Eikonal equation parameterized in celerity, 67th Annual Internat. Mtg., Soc. Expl. Geophys., Expanded Abstracts, 1774-1777.

Podvin, P., and Lecomte, I., 1991, Finite-difference computation of traveltimes in very contrasted velocity models: a massively parallel approach and its associated tools: Geophys. J. Int., **105**,271-284.

Qian, J., and Symes, W.W., 2002, An adaptive finite-difference method for traveltimes and amplitudes: Geophysics, **67**,167-176.

Qin,F., Luo, Y., Olsen,K.B., Cai, W. and Schuster,G.T., 1992, Finite-difference solution of the Eikonal equation along expanding wavefront: Geophysics, **57**,478-487.

Rawlinson, N. and Sambridge, M., 2004, Wave front evolution in strongly heterogeneous layered media using the fast marching: Geophys. J. Int., **156**,631-647.

Reshef, M., and Kosloff, D., 1986, Migration of common shot gathers: Geophysics, **51**, 324-331.

Sethain, J.A., and Vladimirsky, A., 2000, Fast methods for the Eikonal and related Hamilton-Jacobi equations on unstructured meshes: Proc. Nat. Acad. Sci., **97**, 5699-5703.

Schneider, W.A.J., Ranzinger, K.A., Balch, A.H. and Kruse, A., 1992, A dynamic programming approach to first arrival traveltime computation in media with arbitrarily distributed velocities, Geophysics, **57**,39-50.

Sun, Y. and Fomel, S., 1998a Fast-marching Eikonal solver in the tetragonal coordinates: 68^h Ann. Internat. Mtg. Soc. Expl. Geophys., Expanded Abstracts, 1949-1952.

Sun, Y. and Fomel, S., 1998b Fast-marching Eikonal solver in the tetragonal coordinates, SEP-**97**, 241-250.

Tsai, Y.R., Cheng, L.T., Osher, S. and Zhao, H.K., 2003, Fast Sweeping Algorithms for a Class of Hamilton-Jacobi Equations*:* SIAM Journal on Numerical Analysis, **41**, 673-694.

Vidale,J., 1988, Finite-difference calculation of traveltimes, Bull. Seism.Soc.Am., **78**,2062-2076.

Vidale,J., 1990, Finite-difference calculation of traveltimes in three dimensions, Geophysics, **55**, 521-526.

Zhao, H.K., 2003, Fast sweeping method for Eikonal equations: to appear in Math. Comp.

Zhao, P., 1996, An efficient computer program for wavefront calculation by the finite-difference method, Computers & Geosciences, **22**, 239-251.

FIGURES

Figure 1. The update procedure of FD for t_C. The travel times at A and B are known. (d) is diffraction wave from B to C (Eq. (12)), (t) transmission wave (Eq.(6)) and (h) is head wave along AC(Eq.(11)).

Figure 2. Sixteen potential arrivals are calculated which cover all possible ray paths. The one with the minimum travel time is selected as the first arrival. The black dots denote points timed already and the hollow circle will be timed from the traveltimes at the black dots.

Figure 3. The arrival time at point E is computed from (a) A, B and D, (b) A, B and C, and (c) A, D and C. The traveltimes at point A, B , C and D are known and at point E unknown.

Figure 4. Wavefronts(at 2 s intervals) in a constant medium of 6000m/s(unit is second). Receivers are denoted by triangles.

Figure 5. Traveltime errors between numerical and analytical solutions for a constant velocity medium: a) traveltime error and b) percent error.

Figure 6. The traveltime difference between numerical and analytical solution at the 21 receivers shown in Figure 4.

Figure 7. a) Traveltime contours (in seconds); b) relative error (in %) between eikonal solver and analytic solution in a linear velocity gradient medium (vertical gradient of 0.1 s^{-1} with a velocity of 4000 m/s at the surface). The spacing is 125 m in both X- and Z-directions.

Figure 8. The traveltime differences (Δt) between numerical and analytic solutions at the surface Z= 0 with four different spacings: 1000 (red solid line), 500(red dashed line), 250(blue dashed

line) and 125m (blue solid line). The velocity model is a uniform velocity gradient medium (vertical gradient of 0.1 s^{-1} with a velocity of 4000 m/s at the surface).

Figure 9. The left panel: rms error between numerical and analytic solutions against grid spacing; The right panel: elapsed CPU times vs. the number of grid points N for a linear increasing velocity model with vertical gradient of 0.1 s^{-1} and a velocity of 4000 m/s at the surface.

Figure 10. FD traveltime contours (in seconds) superimposed on a saltdome velocity model. The traveltimes can be used in prestack Kirchoff migration.

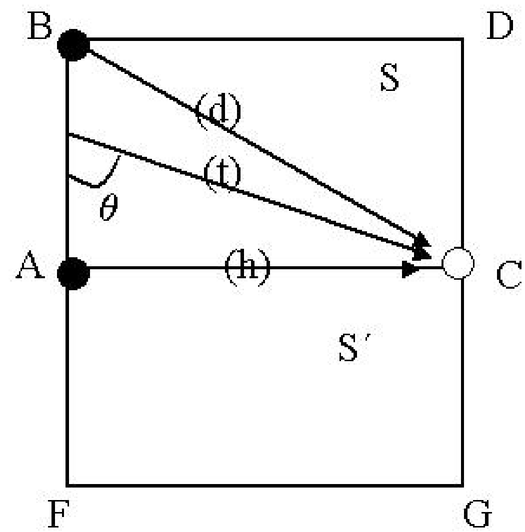

Figure 1. The update procedure of FD for t_C. The travel times at A and B are known. (d) is diffraction wave from B to C (Eq. (12)), (t) transmission wave (Eq.(6)) and (h) is head wave along AC(Eq.(11)).

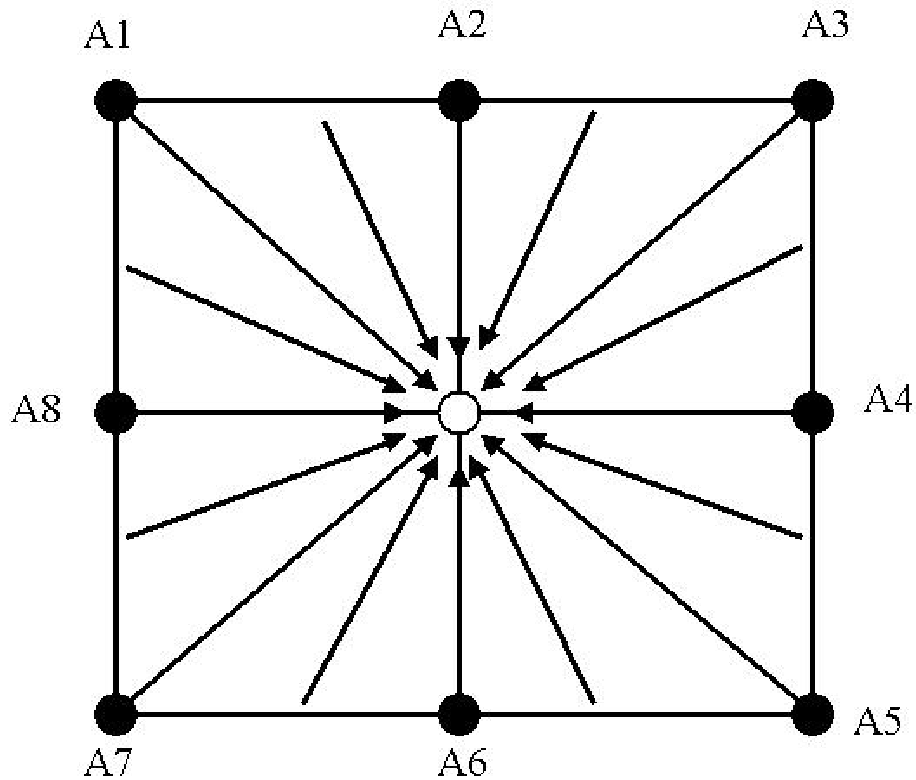

Figure 2. Sixteen potential arrivals are calculated which cover all possible ray paths. The one with the minimum travel time is selected as the first arrival. The black dots denote points timed already and the hollow circle will be timed from the traveltimes at the black dots.

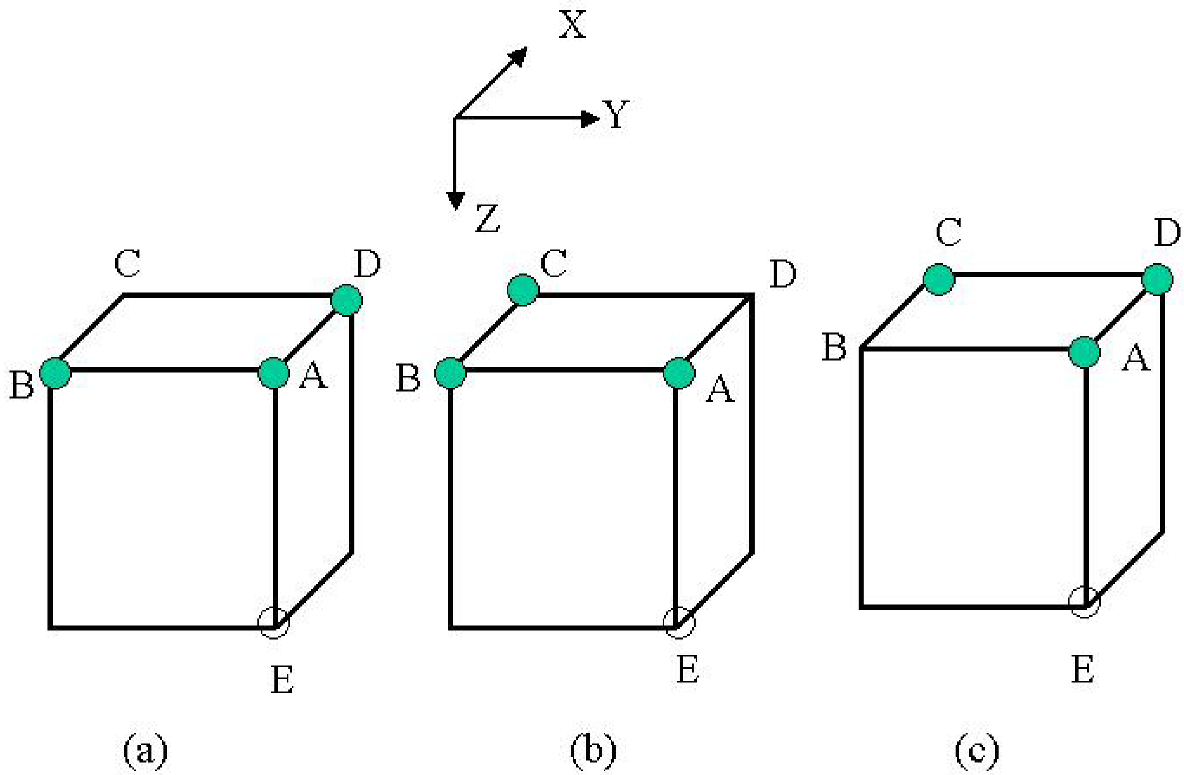

Figure 3. The arrival time at point E is computed from (a) A, B and D, (b) A, B and C, and (c) A, D and C. The traveltimes at point A, B , C and D are known and at point E unknown.

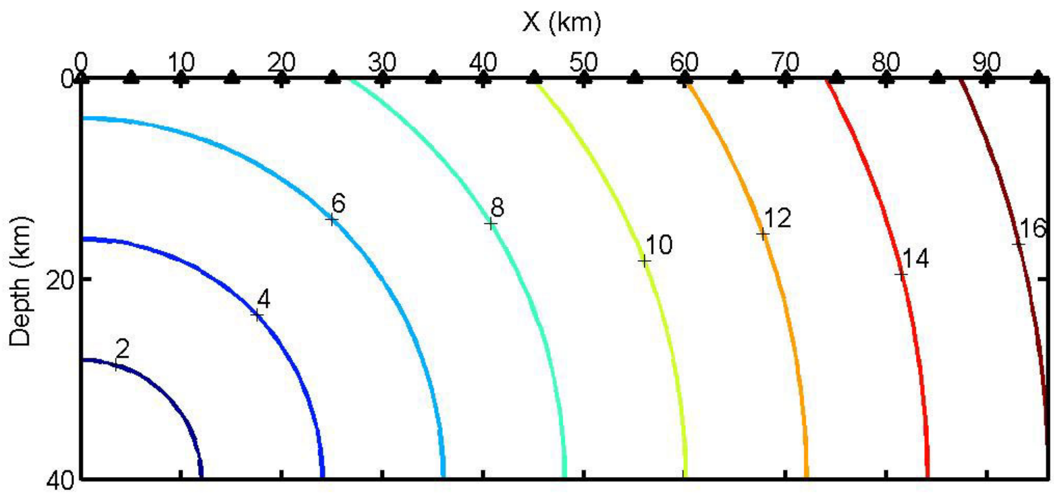

Figure 4. Wavefronts(at 2 s intervals) in a constant medium of 6000m/s(unit is second). Receivers are denoted by triangles.

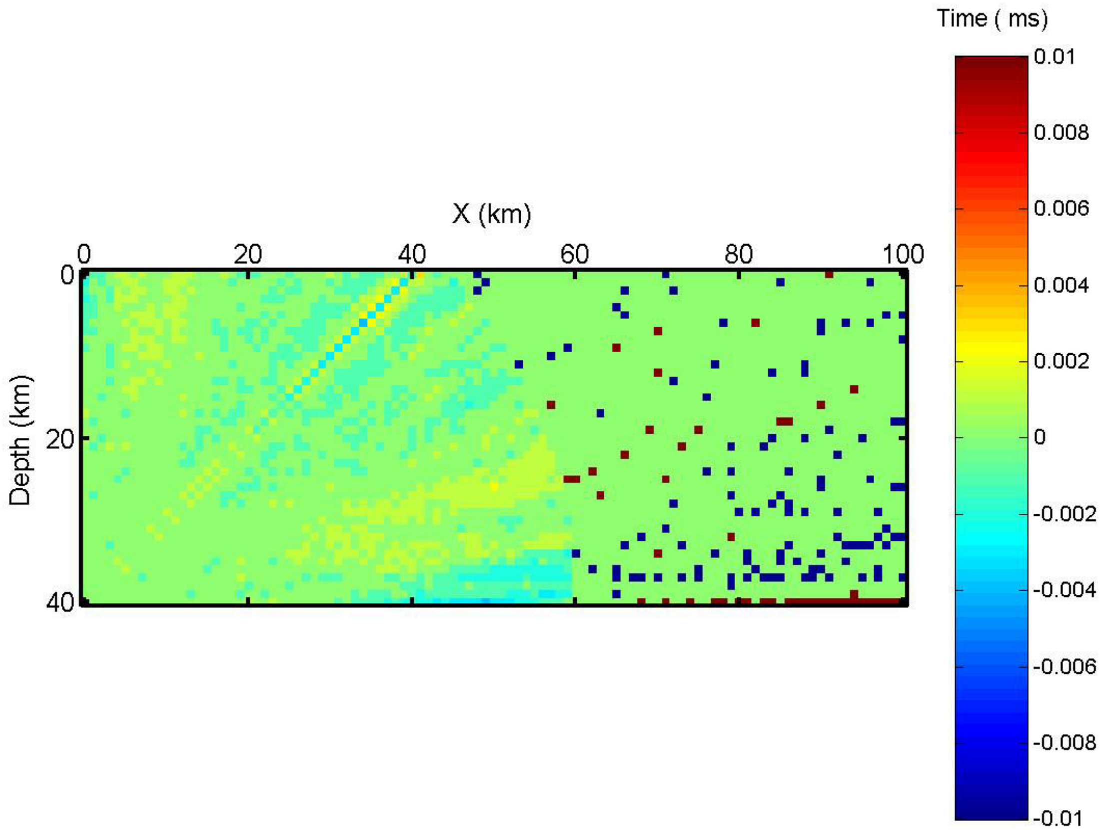

Time (ms)
0.01
0.008
0.006
0.004
0.002
0
-0.002
-0.004
-0.006
-0.008
-0.01
X (km)
0
20
40
60
80
100
Depth (km)
0
20
40

Figure 5. a)

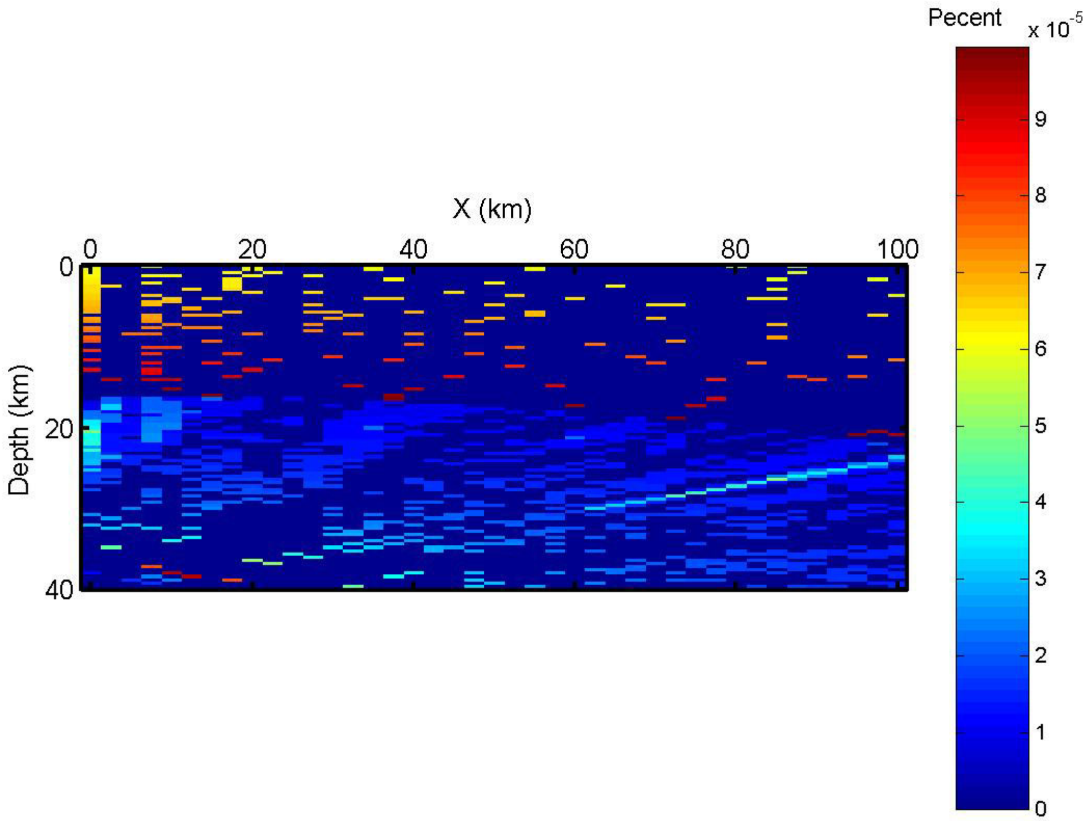

Figure 5. b)

Figure 5. Traveltime errors between numerical and analytical solutions for a constant velocity medium: a) traveltime error and b) percent error.

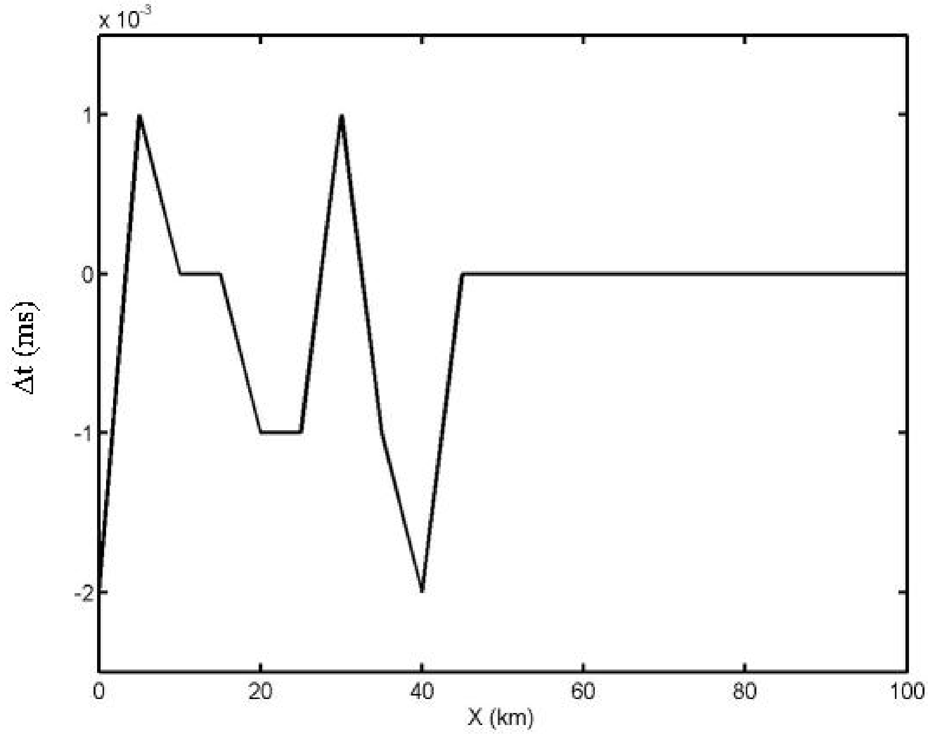

Figure 6. The traveltime difference between numerical and analytical solution at the 21 receivers shown in Figure 4.

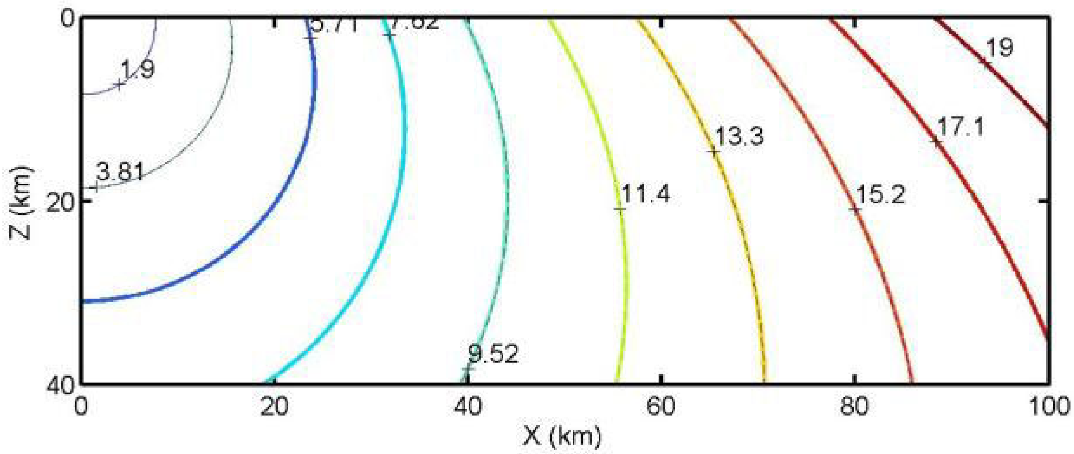
0
20
40
Z (km)
0
20
40
60
80
100
X (km)
1.9
3.81
5.71
7.62
9.52
11.4
13.3
15.2
17.1
19

Figure 4. a)

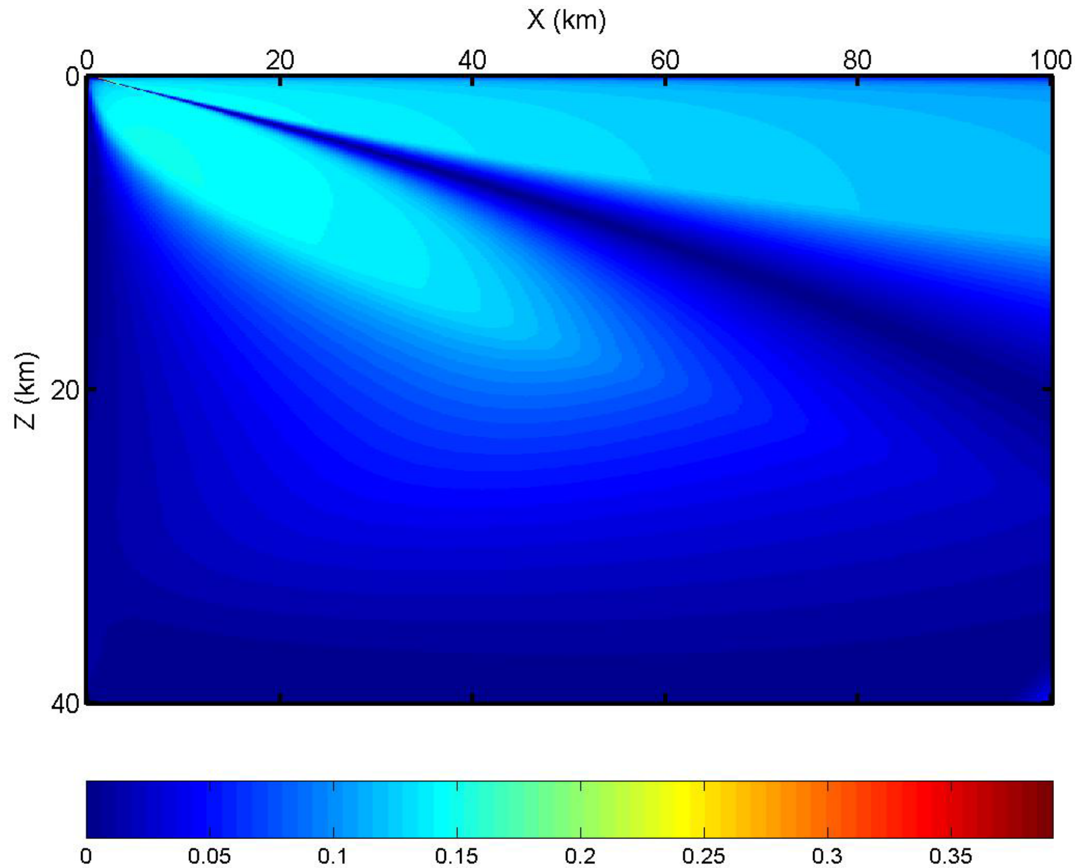

Figure 7. b)

Figure 7. a) Traveltime contours (in seconds); b) relative error (in %) between eikonal solver and analytic solution in a linear velocity gradient medium (vertical gradient of 0.1 s^{-1} with a velocity of 4000 m/s at the surface). The spacing is 125 m in both X- and Z-directions.

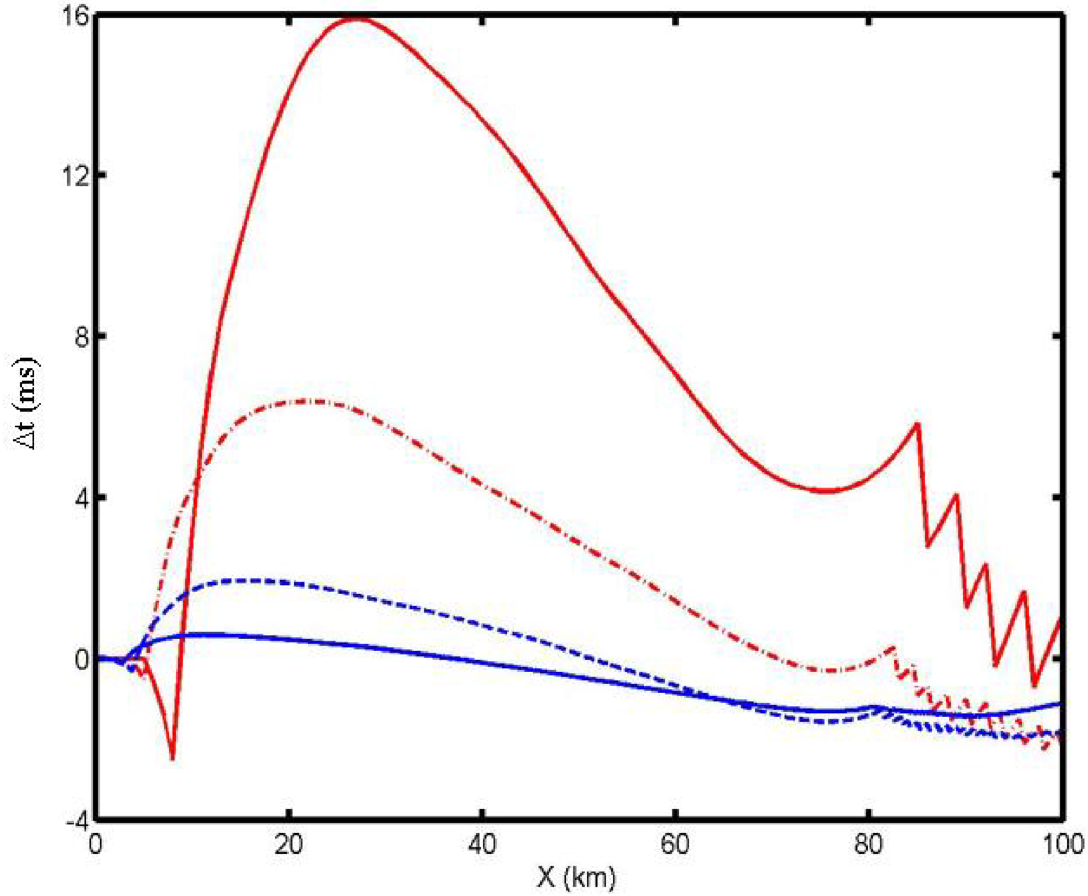

Figure 8. The traveltime differences (Δt) between numerical and analytic solutions at the surface Z= 0 with four different spacings: 1000 (red solid line), 500(red dashed line), 250(blue dashed line) and 125m (blue solid line). The velocity model is a uniform velocity gradient medium (vertical gradient of 0.1 s^{-1} with a velocity of 4000 m/s at the surface).

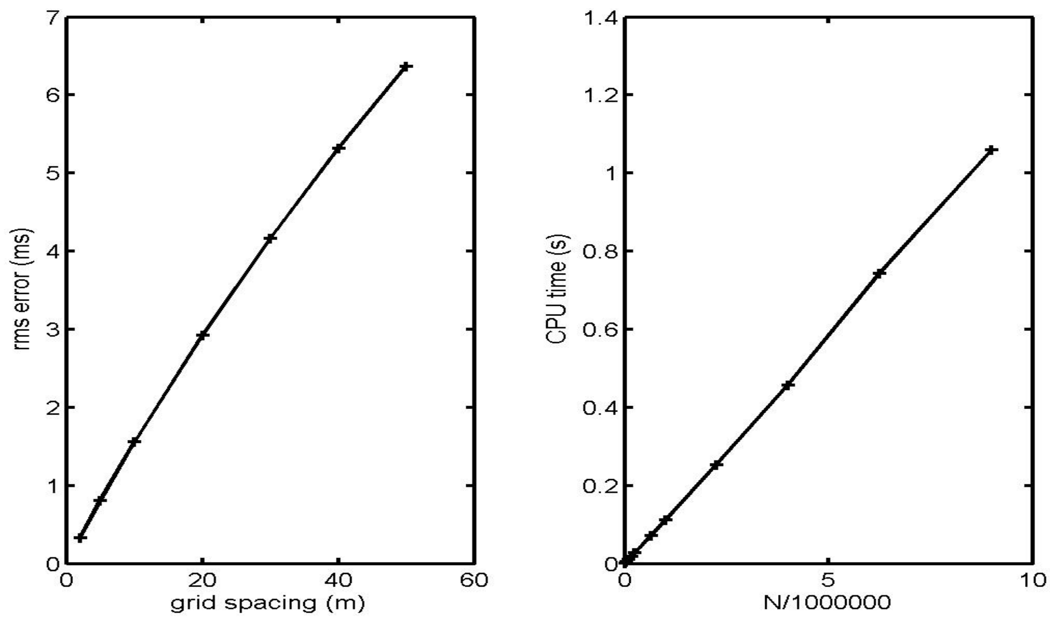

Figure 9. The left panel: rms error between numerical and analytic solutions against grid spacing; The right panel: elapsed CPU times vs. the number of grid points N for a linear increasing velocity model with vertical gradient of 0.1 s^{-1} and a velocity of 4000 m/s at the surface.

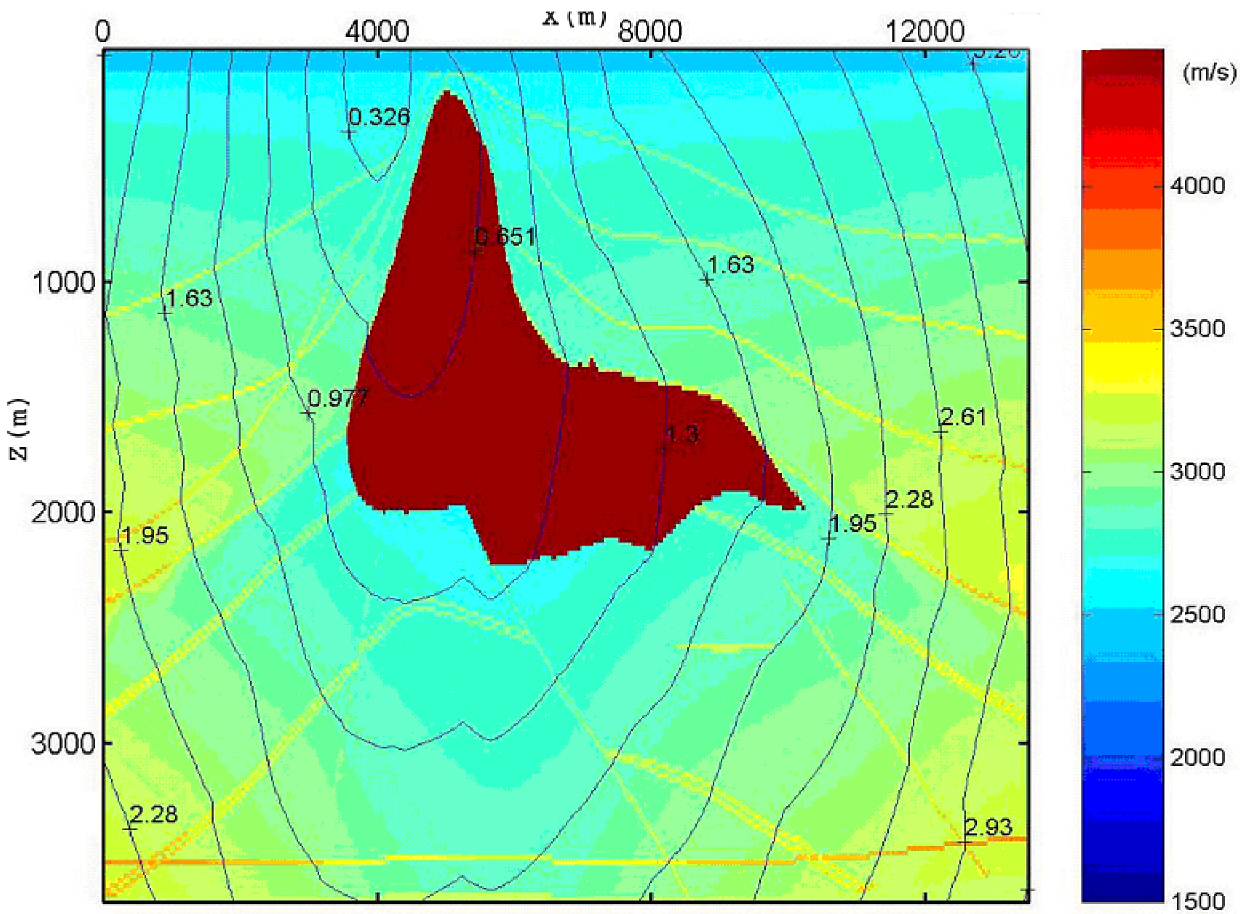

Figure 10. FD traveltime contours (in seconds) superimposed on a saltdome velocity model. The traveltimes can be used in prestack Kirchoff migration.